Cell Communication and Signaling

RESEARCH

Open Access

Nanoscopy reveals integrin clustering reliant on kindlin-3 but not talin-1

Yuanyuan Wu[1], Ziming Cao[1], Wei Liu[1], Jason G. Cahoon[1], Kepeng Wang[1], Penghua Wang[1], Liang Hu[2], Yunfeng Chen[3], Markus Moser[4], Anthony T. Vella[1], Klaus Ley[5], Lai Wen[6*] and Zhichao Fan[1*]

Summary

1. Kindlin-3 but not talin-1 contributes to integrin inside-out signaling induced β2 integrin clustering.
2. The Pleckstrin homology domain of kindlin-3 was critical for its mediated β2 integrin clustering.

Abstract

Background Neutrophils are the most abundant leukocytes in human blood, and their recruitment is essential for innate immunity and inflammatory responses. The initial and critical step of neutrophil recruitment is their adhesion to vascular endothelium, which depends on G protein-coupled receptor (GPCR) triggered integrin inside-out signaling that induces β2 integrin activation and clustering on neutrophils. Kindlin-3 and talin-1 are essential regulators for the inside-out signaling induced β2 integrin activation. However, their contribution in the inside-out signaling induced β2 integrin clustering is unclear because conventional assays on integrin clustering are usually performed on adhered cells, where integrin–ligand binding concomitantly induces integrin outside-in signaling.

Methods We used flow cytometry and quantitative super-resolution stochastic optical reconstruction microscopy (STORM) to quantify β2 integrin activation and clustering, respectively, in kindlin-3 and talin-1 knockout leukocytes. We also tested whether wildtype or Pleckstrin homology (PH) domain deleted kindlin-3 can rescue the kindlin-3 knockout phenotypes.

Results GPCR-triggered inside-out signaling alone can induce β2 integrin clustering. As expected, both kindlin-3 and talin-1 knockout decreases integrin activation. Interestingly, only kindlin-3 but not talin-1 contributes to integrin clustering in the scenario of inside-out-signaling, wherein a critical role of the PH domain of kindlin-3 was highlighted.

Conclusions Since talin was known to facilitate integrin clustering in outside-in-signaling-involved cells, our finding provides a paradigm shift by suggesting that the molecular mechanisms of integrin clustering upon inside-out signaling and outside-in signaling are different. Our data also contradict the conventional assumption that integrin activation and clustering are tightly inter-connected by showing separated regulation of the two during inside-out signaling. Our study provides a new mechanism that shows kindlin-3 regulates β2 integrin clustering and suggests that integrin clustering should be assessed independently, aside from integrin activation, when studying leukocyte adhesion in inflammatory diseases.

*Correspondence:
Lai Wen
lwen@unr.edu
Zhichao Fan
zfan@uchc.edu

Full list of author information is available at the end of the article

© The Author(s) 2024. **Open Access** This article is licensed under a Creative Commons Attribution-NonCommercial-NoDerivatives 4.0 International License, which permits any non-commercial use, sharing, distribution and reproduction in any medium or format, as long as you give appropriate credit to the original author(s) and the source, provide a link to the Creative Commons licence, and indicate if you modified the licensed material. You do not have permission under this licence to share adapted material derived from this article or parts of it. The images or other third party material in this article are included in the article's Creative Commons licence, unless indicated otherwise in a credit line to the material. If material is not included in the article's Creative Commons licence and your intended use is not permitted by statutory regulation or exceeds the permitted use, you will need to obtain permission directly from the copyright holder. To view a copy of this licence, visit http://creativecommons.org/licenses/by-nc-nd/4.0/.

Keywords Neutrophil adhesion, β_2 integrin, Integrin clustering, Kindlin-3, Talin-1, STORM

Introduction

Neutrophils are the most abundant circulating leukocytes in human blood and form a primary line of defense against pathogens [1, 2]. Congenital impairments in neutrophil function, such as those that occur in leukocyte adhesion deficiency syndromes, lead to life-threatening infections [3, 4]. The primary cause of fatal infections in individuals undergoing allogeneic hematopoietic stem cell transplantation is the delayed recovery of neutrophils [5]. Neutrophils also play a crucial role in non-infectious inflammatory scenarios, such as injury-induced sterile inflammation [6, 7] and autoimmune conditions like rheumatoid arthritis [8, 9], multiple sclerosis [10, 11], and systemic lupus erythematosus [12]. Neutrophils circulate in the bloodstream but mainly fulfill their tasks outside the vascular system. Their exit from the circulation towards sites of inflammation follows a well-characterized adhesion cascade, including leukocyte rolling, arrest, intravascular crawling, and transendothelial migration [13–15].

β_2 integrins are essential for multiple steps of the leukocyte recruitment cascade [15–17]. The interaction of lymphocyte function-associated antigen 1 (LFA-1, $\alpha_L\beta_2$ integrin, CD11a/CD18) and macrophage-1 antigen (Mac-1, $\alpha_M\beta_2$ integrin, CD11b/CD18) with endothelial intercellular adhesion molecules (ICAMs) are crucial for human neutrophil arrest [18, 19] — the firm adhesion on vascular endothelium. Neutrophil arrest can be induced by chemoattractant N-formylmethionine-leucyl-phenylalanine (fMLP) [20] and chemokine interleukin 8 (IL-8) [21], which both trigger G protein-coupled receptor (GPCR)-initiated integrin inside-out signaling [22]. Upon inside-out signaling stimulation, β_2 integrins undergo activation to up-regulate their ligand binding affinity through conformational changes in their ectodomain [23, 24]. Meanwhile, clustering of β_2 integrins could also occur to increase their avidity of binding where cooperative strength supports larger forces compared to sporadic integrins [25–28]. β_2 integrin activation [19, 29–31] and clustering [26–28] both significantly contribute to neutrophil adhesion. Previous studies, including ours, showed the conformational changes of β_2 integrin activation [19, 32, 33] and the clustering of activated β_2 integrins [19, 32] during neutrophil adhesion. However, it is unclear whether the integrins are already clustered on circulating neutrophils, and, if so, whether the integrin clustering is triggered by the inside-out signaling. In this study, we used super-resolution stochastic optical reconstruction microscopy (STORM), which provides a ~ 20-nm resolution to visualize and quantify integrin clustering to delineate β_2 integrin clustering induced by inside-out signaling for the first time.

Kindlin-3 and talin-1 are critical for neutrophil β_2 integrin activation [34–39]. They both bind to the cytoplasmic tail of β_2 integrin, where they cooperate to promote full activation of β_2 integrin [40–43]. The involvement of kindlin and talin in integrin clustering has been studied in various systems. For instance, it was shown that talin is a critical regulator of LFA-1 clustering in human T cells [44] and is involved in the formation of cluster-like structures like focal adhesions [45–48] and podosomes [49] in adherent cells. In biomimetic giant unilamellar vesicles in vitro, both talin and kindlin induce $\alpha_{IIb}\beta_3$ integrin clustering [50]. Kindlin-3-null T cells display defective $\alpha_L\beta_2$ clustering after T-cell receptor stimulation [51]. Kindlin-3 is essential for clustering integrins within podosomes of osteoclasts [52], while its homolog kindlin-2 is important for $\alpha_{IIb}\beta_3$ integrin clustering in Chinese hamster ovary cells [53]. However, a limitation of these studies is that they primarily investigated adherent cells in which both integrin inside-out and outside-in signaling (integrin-ligand-binding-triggered) contributed to integrin clustering, making it impossible to discriminate between both signals. To determine whether kindlin-3 and talin-1 are involved in β_2 integrin clustering induced by inside-out signaling alone, we established a method to independently observe neutrophil inside-out signaling and used STORM to visualize β_2 integrin clustering on kindlin-3 and talin-1 knockout (KO) HL60 cells. Surprisingly, we found that kindlin-3 but not talin-1 is critical for integrin clustering in the scenario of GPCR-triggered inside-out signaling. Since talin was known to facilitate integrin clustering in outside-in-signaling-involved cells, as introduced above, our finding provides a paradigm shift by suggesting that the molecular mechanisms of integrin clustering upon inside-out signaling and outside-in signaling are separated. Our data also contrasts the conventional wisdom that integrin activation and clustering are tightly inter-connected by showing separated regulation of the two during inside-out signaling. Targeting inside-out integrin clustering-specific molecules may provide a new strategy for treating inflammatory diseases by improving treatment specificity and reducing the side effects observed in pan-integrin-blocking therapies [54].

Results

Kindlin-3 and talin-1 deficiency impair $\beta_2$integrin activation on HL60 cells

An in vitro cell model of neutrophils was established by treating CXCR2-expressing HL60 cells (HL60-2) [55] with 1.3% DMSO for seven days to stimulate their

differentiation to neutrophil-like cells. In some cells, kindlin-3 [39] or talin-1 [37] were knocked out beforehand using CRISPR-Cas9, while β_2 integrin knockout (β_2-KO) HL60-2 cells [37] were used as a negative control.

To confirm the crucial role of kindlin-3 and talin-1 in β_2 integrin activation, we took advantage of conformation-specific antibodies mAb24 [56] and KIM127 [57]: mAb24 binds to an epitope in the β_2 I-like domain and reports the high-affinity (H^+) conformation [58], while KIM127 binds to an epitope in the extended knee of β_2 integrin, indicating the extended (E^+) conformation [59]. Notably, mAb24 and KIM127 do not interfere with each other or inhibit ligand binding [19]. Using flow cytometry, we found that the mAb24 medium fluorescence intensity (MFI) on the cell surface increased by 5.1-fold after IL-8 stimulation (Fig. 1A) and 4.3-fold after fMLP stimulation (Fig. 1C) in wild-type (WT) cells compared to vehicle controls. In strong contrast, kindlin-3 knockout (K3-KO) and talin-1 knockout (TLN1-KO) cells revealed almost no mAb24 binding, which was comparable to β_2-KO cells (Fig. 1A, C). The results are consistent with previous findings that both kindlin-3 and talin-1 are necessary for β_2 integrin headpiece opening [23, 34]. In all groups, IL-8 and fMLP treatments induced no or minimal changes in overall expression of β_2 integrin (CD18) (Fig. 1E, F); there was also no significant change in GPCRs CXCR2 (for IL-8) or FPR1 (for fMLP) expression on K3-KO and TLN1-KO cells compared to WT controls (Fig. 1G, H), ruling out that the integrin activation defects observed in K3-KO and TLN1-KO cells were due to defects in β_2 integrin or GPCR expression. Consistent with previous studies [34, 37], KIM127 binding was completely abolished in TLN1 KO cells, while it was significantly increased in WT cells after IL-8 and fMLP stimulation (Fig. 1B, D). Surprisingly, KIM127 binding was strongly inhibited in Kindlin-3 KO cells after IL-8 stimulation (Fig. 1B) and completely abolished after fMLP stimulation (Fig. 1D). This indicates that similar to talin-1, kindlin-3 is critical for both β_2 integrin headpiece opening and extension, which is consistent with observations made in Hoxb8 cell-derived talin-1 and kindlin-3 KO neutrophils upon Tumor necrosis factor α (TNFα) and phorbol 12-myristate 13-acetate (PMA) stimulation [60]. These challenged the previous thought in the field that kindlin-3 is only important for β_2 integrin headpiece opening but not extension [33, 34].

Kindlin-3 but not talin-1 is critical for LFA-1 and Mac-1 clustering

To assess β_2 integrin clustering after inside-out signaling while avoiding outside-in signaling, we kept differentiated HL60-2 cells in suspension and incubated them with vehicle control, IL-8, or fMLP, and fixed them for STORM imaging to quantify molecular clustering [32, 61–63]. These cells do not interact with endothelial ICAMs, and there is no involvement of integrin outside-in signaling, which contrasts with previous studies using spreading neutrophils [64–66]. STORM was used

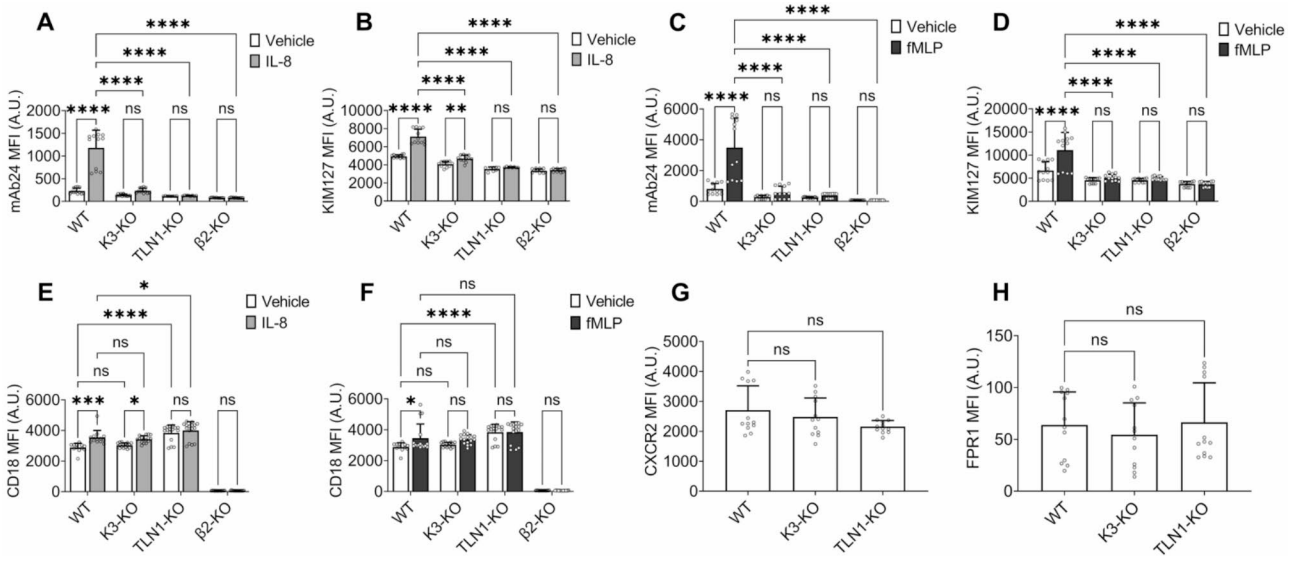

Fig. 1 Kindlin-3 and talin-1 are essential for β_2 integrin activation. Wildtype (WT), kindlin-3 knockout (K3-KO), talin-1 knockout (TLN1-KO), and β_2 integrin knockout (β_2-KO) CXCR2-expressing HL60 (HL60-2) cells were differentiated to neutrophil-like cells. **A**-**D**, β_2 integrin activation was quantified by flow cytometry using conformation-specific antibodies mAb24 (**A**, **C**) and KIM127 (**B**, **D**) with or without IL-8 (**A**-**B**) or fMLP (**C**-**D**) stimulation. **E**-**F**, Total β_2 integrin expression was quantified by flow cytometry using antibody TS1/18 with or without IL-8 (**E**) or fMLP (**F**) stimulation. **G**-**H**, Expression of CXCR2 and FPR1 on cells. MFI, median fluorescence intensity. Means ± SD, $n = 12$ repeats from 3 individual experiments in **A**-**D** and **G**-**H**, $n = 16$ repeats from 4 individual experiments in **E**-**F**. ns $p > 0.05$; *$p < 0.05$; **$p < 0.01$; ***$p < 0.001$; ****$p < 0.0001$ by two-way ANOVA in **A**-**F** and one-way ANOVA in **G**-**H** followed by Tukey's multiple comparison test

to quantify the clustering of LFA-1 and Mac-1 on neutrophil-like HL60-2 cells. We found that both IL-8 and fMLP stimulation effectively induced LFA-1 clustering on WT HL60-2 cells compared to vehicle controls (Fig. 2A-C, S1 A-F). Quantitative analysis showed that the LFA-1 cluster number was increased from ~50 to ~100 per cell after IL-8 (Fig. 2J, L) or fMLP (Fig. 2K, M) stimulation. However, IL-8 or fMLP stimulation did not induce LFA-1 clustering on K3-KO HL60-2 cells (Fig. 2D-F, S1 G-I). The cluster number remained at ~50 per cell after IL-8 (Fig. 2J) or fMLP (Fig. 2K) stimulation. These suggested integrin inside-out signaling already induces LFA-1 clustering, which depends on kindlin-3.

We also tested LFA-1 clustering on TLN1-KO cells. In discrepancy to our original hypothesis that talin is essential for integrin clustering, which was seen in adhered cells, both IL-8 and fMLP stimulation facilitated LFA-1 clustering in TLN1-KO cells (Fig. 2G-I, S1 M-R). Quantitative analysis showed that the LFA-1 cluster number was increased from ~50 to ~250 or 220 per cell after IL-8 (Fig. 2L) or fMLP (Fig. 2M) stimulation, respectively, indicating talin-1 is not required for LFA-1 clustering upon inside-out signaling.

Our STORM imaging of Mac-1 showed results similar to those of LFA-1 (Fig. 3). IL-8 and fMLP stimulation both significantly increased Mac-1 cluster number from ~150 to ~300–400 per WT HL60-2 cell (Fig. 3A-C, J-M, S2 A-F), did not increase Mac-1 cluster number on K3-KO HL60-2 cells (remain ~100 per cell, Fig. 3D-F, J-K, S2 G-L), and significantly increased Mac-1 cluster number from ~100 to ~250–350 per TLN1-KO HL60-2 cell (Fig. 3G-I, L-M, S2 M-R).

The cluster number increase may contribute to the increase of integrin surface expression after chemoattractant stimulation. To compensate for this influence, we normalized the cluster number to the molecular localization number we acquired from each cell (Figure S5 A-D, S6 A-D) and found a similar trend that IL-8 or fMLP triggered inside-out signaling induces integrin clustering in WT and TLN1-KO but not K3-KO HL60-2 cells. We also quantified the cluster size (Figure S5 E-H, S6 E-H) and found that chemoattractant stimulation did not always induce changes in cluster size. We did not find

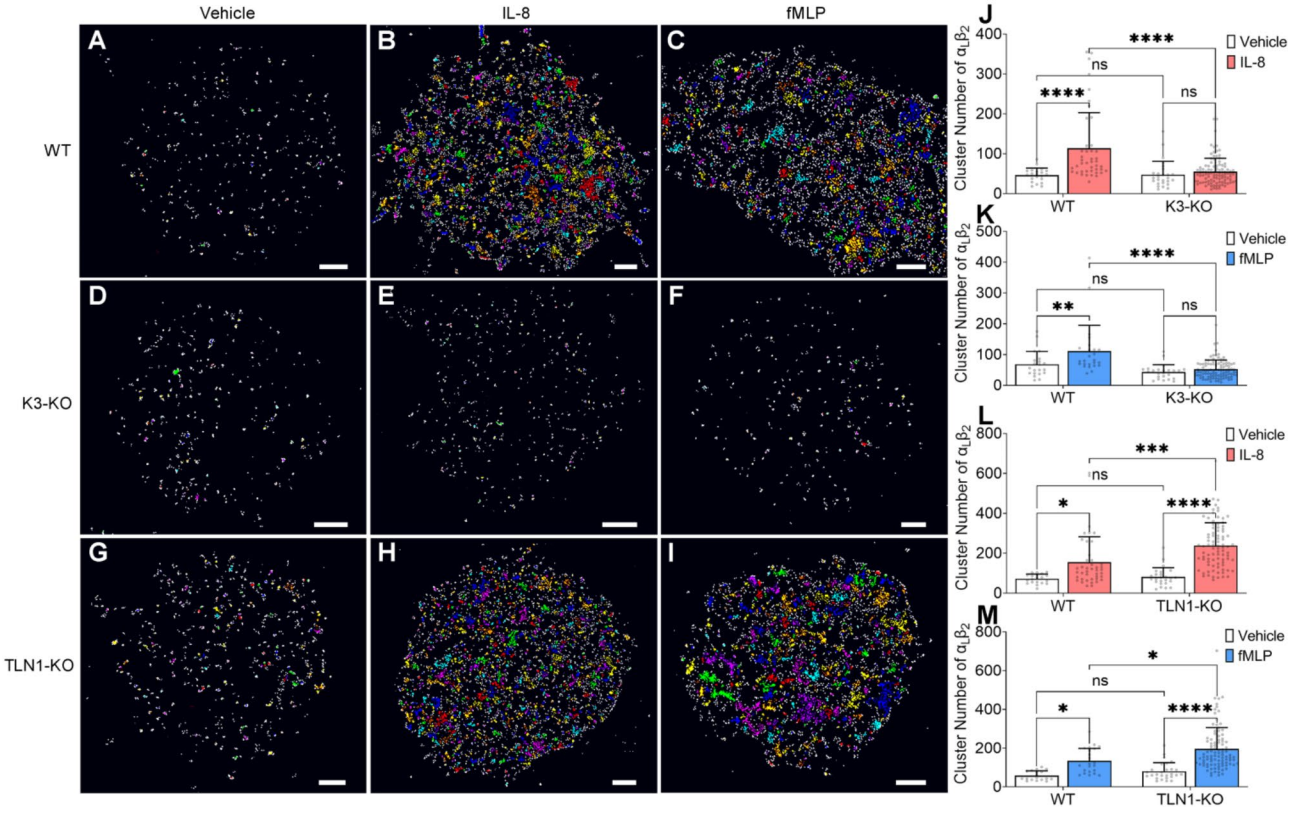

Fig. 2 Kindlin-3 but not talin-1 is critical for $\alpha_L\beta_2$ integrin (LFA-1) clustering. **A**-**I**, Representative STORM images of integrin α_L on wildtype (WT, **A**-**C**), kindlin-3 knockout (K3-KO, **D**-**F**), and talin-1 knockout (TLN1-KO, **G**-**I**) differentiated HL60-2 cells without (**A**, **D**, **G**) or with IL-8 (**B**, **E**, **H**) or fMLP (**C**, **F**, **I**) stimulation after clustering analysis using Voronoi diagrams. Adjacent clusters are distinguished by different colors. Non-clustered α_L are shown as gray dots. Scale bars are 1 μm. **J**-**M**, The number of clusters per WT, K3-KO (**J**-**K**), or TLN1-KO (**L**-**M**) HL60-2 cell without or with IL-8 (**J**, **L**) or fMLP (**K**, **M**) stimulation. Means ± SD ($n \geq 50$ cells from 4 individual experiments). ns, $p > 0.05$; * $p < 0.05$; ** $p < 0.01$; **** $p < 0.0001$, by two-way ANOVA followed by Tukey's multiple comparison test

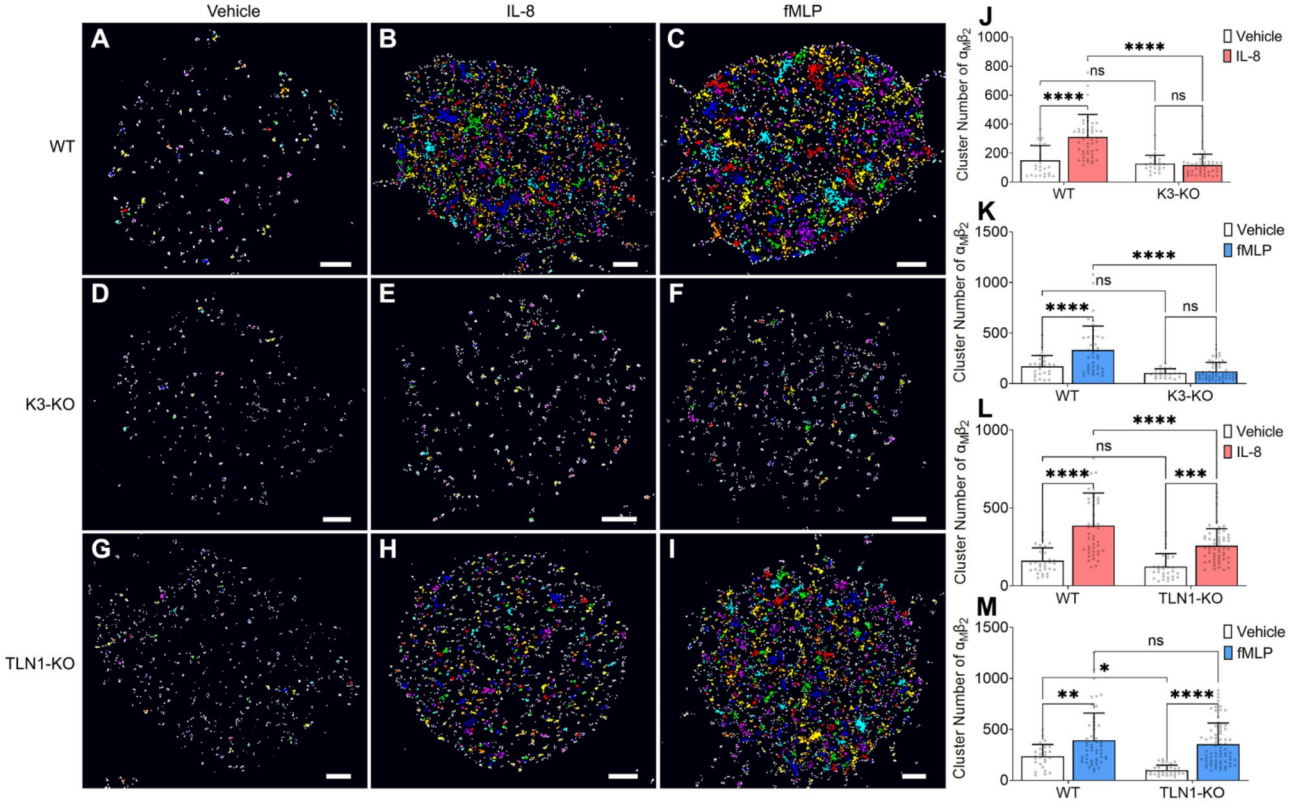

Fig. 3 Kindlin-3 but not talin-1 is important for $\alpha_M\beta_2$ integrin (Mac-1) clustering. **A**-**I**, Representative STORM images of integrin α_M on wildtype (WT, **A**-**C**), K3-KO (**D**-**F**), and TLN1-KO (**G**-**I**) differentiated HL60-2 cells without (**A**, **D**, **G**) or with IL-8 (**B**, **E**, **H**) or fMLP (**C**, **F**, **I**) stimulation after clustering analysis using Voronoi diagrams. Adjacent clusters are distinguished by different colors. Non-clustered α_M were shown as gray dots. Scale bars are 1 μm. **J**-**M**, The number of clusters per WT, K3-KO (**J**-**K**), or TLN1-KO (**L**-**M**) HL60-2 cell without or with IL-8 (**J**, **L**) or fMLP (**K**, **M**) stimulation. Means ± SD ($n \geq 50$ cells from 3 individual experiments). ns $p > 0.05$; * $p < 0.05$; ** $p < 0.01$; *** $p < 0.001$; **** $p < 0.0001$ by two-way ANOVA followed by Tukey's multiple comparison test

a consistent variation tendency in cluster size between groups. Overall, these results indicated that both LFA-1 and Mac-1 clustering upon integrin inside-out signaling requires kindlin-3 but not talin-1.

Kindlin-3 pleckstrin Homology (PH) domain is required for LFA-1 and Mac-1 clustering

To further investigate the mechanism of how kindlin-3 regulates β_2 integrin clustering, we transduced the PH domain-deleted kindlin-3 mutant (ΔPH-K3) or WT kindlin-3 (WT-K3) to K3-KO HL60-2 cells [39] and assessed LFA-1 and Mac-1 clustering using STORM imaging. As expected, WT-K3 transduction rescued the up-regulation of LFA-1 clustering triggered by IL-8 or fMLP stimulation (Fig. 4A-C, S3 A-F), allowing the LFA-1 cluster number to be significantly increased from ~70 to ~150 per cell (Fig. 4G, H). In comparison, IL-8 or fMLP failed to up-regulate LFA-1 clustering on ΔPH-K3-transduced cells (Fig. 4D-F, S3G-L), where the LFA-1 cluster number remained at ~70 per cell (Fig. 4G, H).

Mac-1 clustering also showed similar results (Fig. 5). Specifically, IL-8 or fMLP stimulation significantly increased Mac-1 cluster number from ~200 to ~350 or 250, respectively, per WT-K3 HL60-2 cell (Fig. 5A-C, G-H, S4 A-F), but failed to do so on ΔPH-K3 HL60-2 cells (remained at ~200 per cell, Fig. 5D-F, G-H, S4 G-L).

Similar to what we analyzed for K3 KO and TLN1 KO HL60-2 cells, we also quantified normalized cluster number and cluster size in WT-K3 and ΔPH-K3 HL60-2 cells (Fig. S7) and found that PH domain deletion in kindlin-3 interrupted normalized LFA-1 and Mac-1 cluster number but not cluster size. Overall, these results showed that PH domain deletion in kindlin-3 interrupted LFA-1 and Mac-1 clustering, suggesting a crucial role of the PH domain in kindlin-3-mediated β_2 integrin clustering.

Discussion

Leukocyte adhesion requires both integrin activation and clustering, which are conventionally believed to be closely linked. However, it remains unclear whether integrin inside-out signaling, besides integrin activation, also triggers clustering. Bridging this gap, our study showed that the chemoattractant-triggered integrin inside-out signaling induces not only the activation but also the clustering of β_2 integrins on human neutrophil-like (HL60) cells. We further found that talin-1 is dispensable

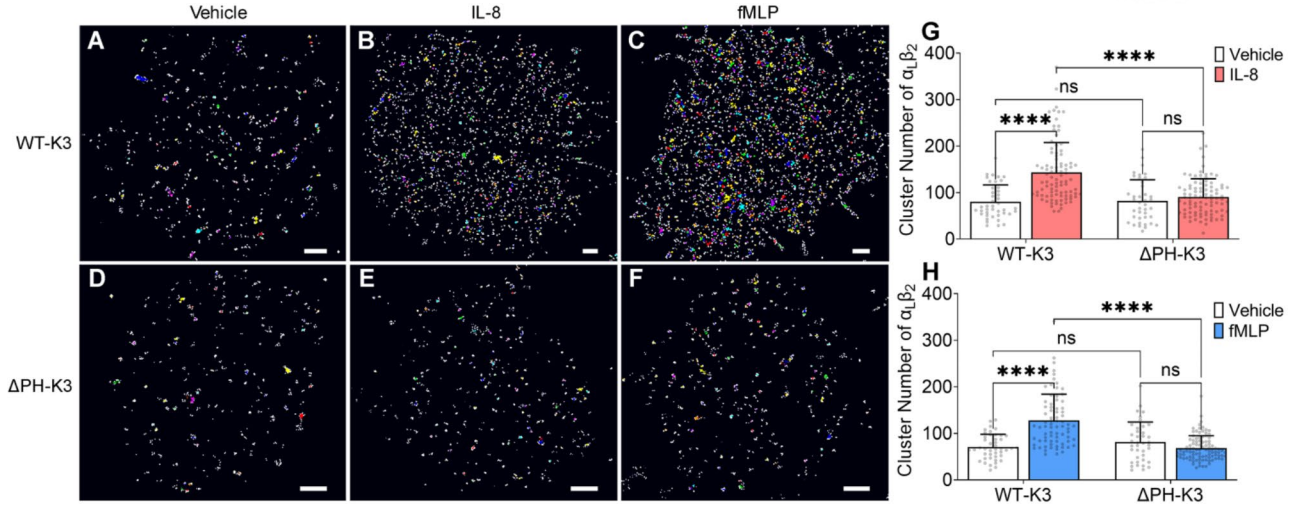

Fig. 4 PH domain in kindlin-3 is required for $\alpha_L\beta_2$ (LFA-1) clustering. **A**-**F**, Representative STORM images of integrin α_L on differentiated HL60-2 cells containing wildtype kindlin-3 (WT-K3, **A**-**C**) and PH domain-deleted kindlin-3 (ΔPH-K3, **D**-**F**) without (**A**, **D**) or with IL-8 (**B**, **E**) or fMLP (**C**, **F**) stimulation after clustering analysis using Voronoi diagrams. Adjacent clusters are distinguished by different colors. Non-clustered α_L are shown as gray dots. Scale bars are 1 μm. **G**-**H**, The number of clusters per WT-K3 or ΔPH-K3 HL60-2 cell without or with IL-8 (**g**) or fMLP (**H**) stimulation. Means ± SD ($n \geq 75$ cells from 3 individual experiments). ns $p > 0.05$; ** $p < 0.01$; **** $p < 0.0001$ by two-way ANOVA followed by Tukey's multiple comparison test

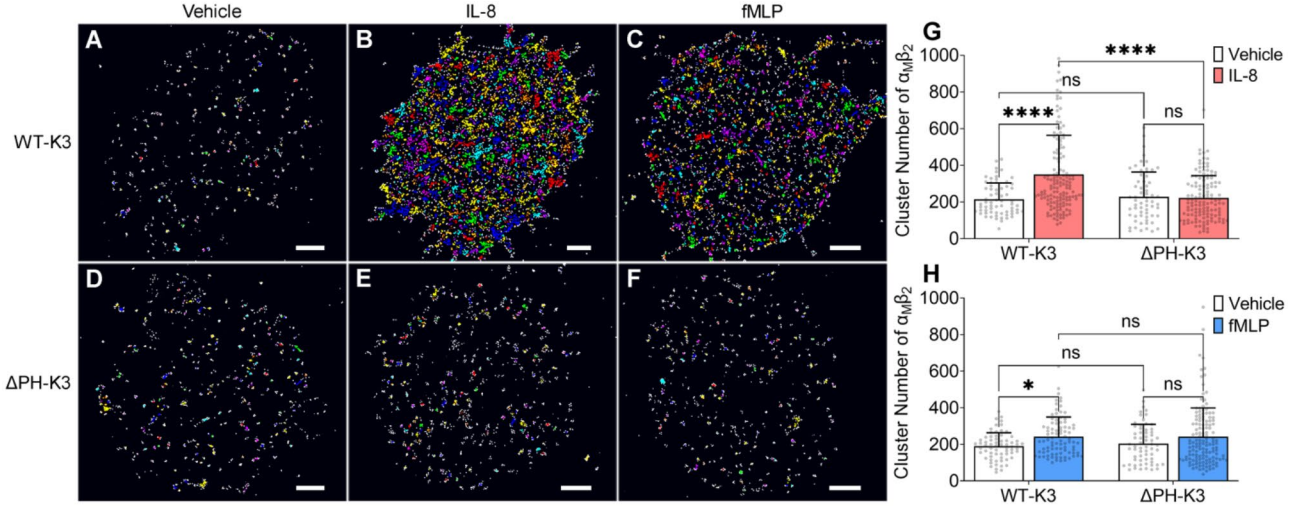

Fig. 5 PH domain in kindlin-3 is required for $\alpha_M\beta_2$ integrin (Mac-1) clustering. **A**-**C**, Representative STORM images of integrin α_M on differentiated HL60-2 cells containing wild-type kindlin-3 (WT-K3, **A**-**C**) and PH domain-deleted kindlin-3 (ΔPH-K3, **D**-**F**) without (**A**, **D**) or with IL-8 (**B**, **E**) or fMLP (**C**, **F**) stimulation after clustering analysis using Voronoi diagrams. Adjacent clusters are distinguished by different colors. Non-clustered α_M are shown as gray dots. Scale bars are 1 μm. **G**-**H**, The number of clusters per WT-K3 or ΔPH-K3 HL60-2 cell without or with IL-8 (**G**) or fMLP (**H**) stimulation. Means ± SD ($n \geq 85$ cells from 3 individual experiments). ns $p > 0.05$; * $p < 0.05$; ** $p < 0.01$; **** $p < 0.0001$ by two-way ANOVA followed by Tukey's multiple comparison test

for inside-out signaling induced β_2 integrin clustering, whereas kindlin-3 plays a critical role. These results are in contrast to a recent study that reported that kindlin and talin cooperate in facilitating integrin clustering [50], wherein talin plays a primary role while kindlin is only secondary. Kindlin-2 cooperates with talin to activate integrins and induces cell spreading by directly binding paxillin [67]. Since talin is known to contribute to the formation of cluster-like structures, such as focal adhesions [45–48] and podosomes [49], in adherent spreading cells, our results suggest that the integrin clustering mediated by inside-out signaling and outside-in signaling might involve distinguished molecular mechanisms. Thus, our study advocates for the careful selection of experimental systems to distinguish integrin inside-out and outside-in signaling in future studies addressing integrin clustering.

Our discovery that talin-1 is required only for β_2 integrin activation but not clustering during inside-out signaling suggests that integrin activation and clustering are regulated by different molecular signaling mechanisms.

In support of this, a previous study demonstrated that a voltage-gated potassium channel KV1.3 reinforces neutrophil adhesion without facilitating integrin activation [68], suggesting that its contribution might be only via mediating integrin clustering. The distinctive molecular mechanisms underlying integrin activation and clustering deserve further investigations in the future. Notably, since our study only focuses on integrin inside-out signaling, the possible role of talin-1 in integrin clustering during outside-in signaling still cannot be excluded.

While the importance of kindlin-3 in β_2 integrin activation is increasingly recognized [34], its specific function is still debated. Lefort et al. used cell-permeable constitutively active Rap1a to stimulate integrin activation in HL60 cells and showed that kindlin-3 knockdown only affects β_2 integrin activation to the H^+ but not E^+ conformation [34]. However, another study using kindlin-3 KO neutrophils differentiated from Hoxb8 immortalized progenitor cells showed major defects in both H^+ and E^+ activation of β_2 integrins after TNFα and PMA stimulation [60]. The discrepancy between both studies may be caused by the incomplete KO in the HL60 study. Similarly, our previous work [39] and the current study also showed significant defects in β_2 integrin activation towards both the H^+ and E^+ states on kindlin-3 KO HL60 cells, suggesting that in addition to talin-1, kindlin-3 is also an indispensable regulator for both β_2 integrin headpiece opening and ectodomain extension.

Mutations in the *FERMT3* gene encoding kindlin-3 are responsible for leukocyte adhesion deficiency III (LAD-III), a disease characterized by leukocyte and platelet dysfunction [51, 53, 69]. Clinical research suggests that *FERMT3* mutation results in loss of kindlin-3 expression, which causes strong defects in β_2 integrin-mediated neutrophil adhesion and spreading [70–72]. Mechanistic studies indicate that kindlin-3 deficiency disrupts integrin-involved osteoclast actin cytoskeleton organization and integrin-dependent erythropoiesis [72, 73]. In this context, our study provides a new mechanism of how kindlin-3 regulates leukocyte adhesiveness — not only through integrin activation but, as shown here, also through integrin clustering. This finding provides new insight into the understanding of LAD-III pathogenesis and potentially a novel path for intervention.

Furthermore, it is considered that the PH domain is indispensable for the induction of high-affinity activation of β_2 integrins and kindlin-3 mediated cell adhesion [39, 74, 75]. According to the crystal structure of human full-length kindlin-3 [76], a PH domain is inserted in its F2 subdomain, which displays a binding affinity for phosphoinositide PI [3–5]P3 (PIP3) and induces PIP lipid clustering in bilayer membranes [77, 78]. PIP3 can cluster around PH domains to form stable nanoscale microdomains in cell membranes [79, 80], which perform like a protein-anchoring unit and enhance interactions with proteins [81–84]. In this study, we found the PH domain-deleted kindlin-3 failed to induce general clustering of LFA-1 and Mac-1, as seen in HL60 cells expressing WT kindlin-3. These results demonstrate the importance of the kindlin-3 PH domain to β_2 integrin clustering, with a postulated mechanism that the PH domain facilitates kindlin-3 binding to PIP3 and, in turn, the anchorage of kindlin-3 onto the cell membrane, thereby promoting its capability in mediating integrin clustering.

In summary, our study provides a new mechanism that shows kindlin-3 regulates β_2 integrin clustering upon inside-out signaling through its PH domain and concludes that talin-1 has been mistakenly involved because STORM nanoscopy was needed to resolve their roles, not conventional technologies previously used. Our study also suggests that integrin clustering should be considered an independent process, aside from integrin activation, when studying leukocyte adhesion in inflammatory diseases. Targeting integrin clustering-specific regulating molecules may provide a new strategy to treat inflammatory diseases without affecting integrin activation and basic immune functions.

Materials and methods

Reagents

For flow cytometry, KIM127 was directly labeled by DyLight 550 using DyLight microscale antibody (Ab) labeling kits (catalog no. 84531) from Thermo Fisher Scientific. Allophycocyanin (APC)-conjugated CD11a/CD18 (LFA-1) mouse anti-human mAb24 Ab (catalog no. 363410), Alexa Fluor 700 (AF700)-conjugated mouse anti-human CD18 Ab (catalog no. 302123), Pacific Blue™-conjugated mouse anti-human CXCR2 Ab (catalog no. 320723), APC-conjugated mouse anti-human FPR1 Ab (catalog no. 391609), Pacific Blue™-conjugated mouse anti-human IgG1 Ab (catalog no. 400131), and APC-conjugated mouse anti-human IgG1 Ab (catalog no. 400120) were purchased from BioLegend. For STORM imaging, Alexa Fluor 647 (AF647)-conjugated mouse anti-human CD11a Ab (catalog no. 301218) and AF647-conjugated mouse anti-human CD11b Ab (catalog no. 393109) were purchased from BioLegend, while glucose oxidase from Aspergillus niger (catalog no. G2133), catalase from bovine liver (catalog no. C40), and cysteamine (catalog no. 30070) were purchased from Sigma-Aldrich.

Roswell Park Memorial Institute medium 1640 (RPMI-1640) with (catalog no. 11875-093) or without phenol red (catalog no. 11835-030) and penicillin and streptomycin (catalog no. 15140-122) were purchased from Gibco. Fetal bovine serum (FBS) (catalog no. 100–106) and 25% human serum albumin (HSA) (catalog no. 800 − 120) were purchased from Gemini Bio Products. 1 × phosphate-buffered saline (PBS) without Ca^{2+} and Mg^{2+} (catalog

no. SH30256.02) was purchased from Cytiva. Recombinant human IL-8 was purchased (catalog no. 208-IL-050) from R&D Systems. fMLP (catalog no. 47729), dimethyl sulfoxide (DMSO) (catalog no. D2650), and 0.01% poly-L-lysine solution (catalog no. A-005-C) were purchased from Sigma-Aldrich. 25% Glutaraldehyde (GA) (catalog no. A17876) and 16% paraformaldehyde (PFA) (catalog no. 043368.9 M) were purchased from Thermo Fisher Scientific.

Cell culture and isolation

Kindlin-3 knockout (K3-KO) [39], talin-1 knockout (TLN1-KO) and β_2 integrin knockout (β_2-KO) [37] cell lines were generated by CRISPR-Cas9 from stable CXCR2-expressing HL60 cells [85], K3-KO HL60 cells transfected by wildtype kindlin-3 (WT-K3), or PH domain-deleted kindlin-3 (ΔPH-K3) mutant [39]. HL60 cells were maintained in culture medium (RPMI-1640, 10% FBS, 100 μg/mL penicillin, and 100 μg/mL streptomycin) at 37℃ in a humidified atmosphere, 5% CO_2 incubator. HL60 cells were differentiated with 1.3% dimethyl sulfoxide for 6 ~ 7 days before assays.

10 mL differentiated cells were collected and centrifuged for 5 min at 300 × g and 20℃. After washing with PBS without Ca^{2+} and Mg^{2+} and centrifuging at 550 × g twice, cells were resuspended in RPMI 1640 without phenol red plus 2% HSA and used within 4 h.

Flow cytometry

To test the expression of CD18, CXCR2, and FPR1 in HL60 cells (Fig. 1C, D, G, H), 2.5×10^5/mL cells were stained with 1 μg/mL antibodies in 100 μL of volume. AF700-conjugated CD18 Ab, Pacific Blue™-conjugated CXCR2 Ab, and APC-conjugated FPR1 Ab were used to test the expression of total β_2 integrin, IL-8 receptor, and fMLP receptor. The staining of Pacific Blue™-conjugated IgG1 Ab and APC-conjugated IgG1 Ab were used as isotype controls for CXCR2 Ab and FPR1 Ab. After staining for 10 min, cells were fixed with 1% PFA for 10 min at 4 ℃. Each cell sample was washed with 200 μL PBS and centrifuged at 550 × g twice. After resuspending cells in PBS, cell fluorescence was assessed with an LSRII (BD™) and analyzed with FlowJo software.

For the β_2 integrin activation assay (Fig. 1A, B, E, F), 2.5×10^5/mL HL60 cells were incubated with 1 μg/mL IL-8 or 100 nM fMLP for 10 min at 300 × g vibration and room temperature (RT) in the presence of 0.5 μg/mL APC-conjugated mAb24 and 0.5 μg/mL DyLight 550-labeled KIM127 Ab. Vehicles were added as controls. After the incubation, cells were fixed with 1% PFA for 10 min at 4℃. Each cell sample was washed with 200 μL PBS and centrifuged at 550 × g twice. After resuspending cells in PBS, cell fluorescence was assessed with an LSRII (BD™) and analyzed with FlowJo software.

STORM imaging

A glass-bottomed 8-Well M-Slide imaging chamber (ibidi) was coated with 250 μL 0.01% poly-L-lysine at 4℃ overnight. After 3 washes with ddH_2O, the chamber was ready for seeding cells. 200 μL 5×10^6 /mL cells were stained with 5 μg/mL AF647-conjugated anti-human CD11a or CD11b antibodies and were incubated with vehicle control, 1 μg/mL IL-8, or 100 nM fMLP for 10 min at RT on a plate vibrator (300 rpm) at the same time with antibody incubation. Then, cells were fixed by 200 μL mixture of 0.05% GA and 1% PFA for 10 min at 4 ℃. Centrifuge the plate at 500× RT for 5 min to settle down the cells. After 2 washes with PBS to remove floating cells, samples were ready for imaging.

During STORM imaging, a special buffer will be added to the wells to replace PBS. STORM imaging buffer was prepared within 3 h prior to imaging. The STORM buffer was prepared by gently adding 7 μL GLOX solution (14 mg glucose oxidase and 1 mg catalase dissolved in 500 μL 10 mM Tris with 50 mM NaCl) and 70 μL 1 M cysteamine (77 mg cysteamine and 21 μL HCl in 1 mL ddH_2O, or) into 620 μL of 50 mM Tris with 10 mM NaCl and 10% Glucose [62].

Imaging was performed by using an iX83 Olympus inverted microscope equipped with the SAFe Light module (Abbelight, includes four color lasers, λ=405 nm, 488 nm, 532 nm, and 640 nm), sCMOS fusion cameras (Hamamatsu), and a 100 × NA 1.5 oil objective. The bottom of labeled cells were continuously illuminated by the 647 nm laser during image acquisition. Power on the 647-nm lasers was adjusted to 20% to enable the collection of between 100 and 300 localization blinks per618×618-pixel (97 nm·pixel-1, 60 × 60 μm2) camera frame in the center of the field at appropriate threshold settings. The collection was set to 10,000 frames, yielding 1–3 million localizations.

Clustering image processing

The STORM images of single cells were processed by NEO Analysis (Abbelight). The cluster number on each cell was calculated by Voronoï tessellation [86, 87]. Compared to Density-based spatial clustering analysis with noise (DBSCAN) and K-Ripley functions, the Voronoï tessellation is less sensitive to background noise and has been approved for more accuracy in analyzing molecular clusters in STORM images [84]. Briefly, circles around the most likely centers of each LFA-1 or Mac-1 localization were constructed to define clusters. The maximum diameter of the circles was set to 50 nm, which indicated that two localizations within 50 nm were considered to be in the same cluster. We also defined clusters as having at least 5 LFA-1 or Mac-1 localizations. The average localization density of each cell was set to 28 localizations/μm^2. Then, a threshold of twice the average localization

density was used to determine clusters. To eliminate the effect of different LFA-1 or Mac-1 expression on different cells, we normalized the cluster number to the molecular localization number on each cell and showed the results as cluster number per 10,000 localizations.

Statistics

Statistical analysis was performed using PRISM software (version 9.00, GraphPad Software). Data analysis was performed using one-way ANOVA followed by Tukey's multiple comparison tests (Fig. 1D, H) or two-way ANOVA followed by Tukey's multiple comparison tests (Figs. 1A-C and E-G, 2J-M, 3J-M, 4G-H and 5G-H), which are indicated in figure legends. *P*-values < 0.05 were considered significant statistically.

Supplementary Information

The online version contains supplementary material available at https://doi.org/10.1186/s12964-024-02024-8.

Supplementary Material 1

Acknowledgements

The CXCR2-expressing HL60 cells were a gift from Dr. Ann Richmond at the Vanderbilt University School of Medicine. We acknowledge Dr. Evan Jellison and Ms. Li Zhu in the Flow Cytometry Core at UConn Health for their assistance with flow cytometry. We acknowledge Dr. Bernard L. Cook from UConn School of Medicine for his help with the scientific writing and editing of this manuscript.

Author contributions

Conceptualization: Z.F. Data curation and investigation: Y.W. Methodology: Z.F. Formal analysis: Y.W. and Z.C. Resources and validation: W.L., J.C., K.W., P.W., M.M., K.L., and L.W. Writing – original draft: Y.W. Writing – review & editing: Y.W., P.W., L.H., Y.C., M.M., A.T.V., K.L., L.W., and Z.F. Supervision: Z.F. and L.W.

Funding

National Institutes of Health, National Heart, Lung, and Blood Institute, USA (R01-HL145454, R01-HL174533, and R00-HL153678). National Institute on Aging (The Claude D. Pepper Older Americans Independence Center Award P30-AG024832), National Institute of General Medical Sciences (COBRE P20GM130459). Cystic Fibrosis Foundation (00841I221 and 005693G223). American Heart Association (CDA 942098). Deutsche Forschungsgemeinschaft, Germany (SFB914 TP A01 and DFG MO 927/9 – 1). Startup fund from UConn Health.

Data availability

No datasets were generated or analysed during the current study.

Declarations

Competing interests

The authors declare no competing interests.

Author details

[1]Department of Immunology, University of Connecticut School of Medicine, Connecticut, Farmington 06030, USA
[2]Academy of Integrative Medicine, Shanghai University of Traditional Chinese Medicine, Shanghai 201203, China
[3]Department of Biochemistry and Molecular Biology, Department of Pathology, University of Texas Medical Branch, Galveston, Texas 77555, USA
[4]Institute of Experimental Hematology, School of Medicine, Technical University of Munich, 81675 Munich, Germany
[5]Immunology Center of Georgia, Augusta University, Augusta, Georgia 30912, USA
[6]Department of Pharmacology, University of Nevada School of Medicine, Reno, Nevada 89557, USA

Received: 11 November 2024 / Accepted: 30 December 2024
Published online: 07 January 2025

References

1. Liew PX, Kubes P. The Neutrophil's role during Health and Disease. Physiol Rev. 2019;99:1223–48.
2. Mayadas TN, Cullere X, Lowell CA. The multifaceted functions of neutrophils. Annu Rev Pathol. 2014;9:181–218.
3. Gronloh MLB, Tebbens ME, Kotsi M, Arts JJG, van Buul JD. Intercellular adhesion molecule 2 regulates diapedesis hotspots by allowing neutrophil crawling against the direction of flow. Vasc Biol. 2023;5(1):e230005.
4. Papayannopoulos V. Neutrophil extracellular traps in immunity and disease. Nat Rev Immunol. 2018;18:134–47.
5. Tecchio C, Cassatella MA. Uncovering the multifaceted roles played by neutrophils in allogeneic hematopoietic stem cell transplantation. Cell Mol Immunol. 2021;18:905–18.
6. Kolaczkowska E, Kubes P. Neutrophil recruitment and function in health and inflammation. Nat Rev Immunol. 2013;13:159–75.
7. Wang K, et al. Locally organised and activated Fth1(hi) neutrophils aggravate inflammation of acute lung injury in an IL-10-dependent manner. Nat Commun. 2022;13:7703.
8. Marin-Prida J, et al. The effects of Phycocyanobilin on experimental arthritis involve the reduction in nociception and synovial neutrophil infiltration, inhibition of cytokine production, and modulation of the neuronal proteome. Front Immunol. 2023;14:1227268.
9. Jin L, et al. Low-dose ethanol consumption inhibits neutrophil extracellular traps formation to alleviate rheumatoid arthritis. Commun Biol. 2023;6:1088.
10. Nouri M, Westrom B, Lavasani S. Elevated fecal calprotectin accompanied by intestinal neutrophil infiltration and Goblet Cell Hyperplasia in a murine model of multiple sclerosis. Int J Mol Sci. 2023;24(20):15367.
11. McGinley AM, et al. Interleukin-17A serves a priming role in autoimmunity by recruiting IL-1beta-Producing myeloid cells that promote pathogenic T cells. Immunity. 2020;52:342–e356346.
12. Zhou HY et al. Recent advances in the involvement of epigenetics in the pathogenesis of systemic lupus erythematosus. Clin Immunol. 2023;258:109857.
13. Phillipson M, Kubes P. The neutrophil in vascular inflammation. Nat Med. 2011;17:1381–90.
14. Sadik CD, Kim ND, Luster AD. Neutrophils cascading their way to inflammation. Trends Immunol. 2011;32:452–60.
15. Ley K et al. Neutrophils: New insights and open questions. Sci Immunol. 2018;3(30):eaat4579.
16. Bader A, et al. Molecular insights into Neutrophil Biology from the zebrafish perspective: lessons from CD18 Deficiency. Front Immunol. 2021;12:677994.
17. Yago T, Zhang N, Zhao L, Abrams CS, McEver RP. Selectins and chemokines use shared and distinct signals to activate beta2 integrins in neutrophils. Blood Adv. 2018;2:731–44.
18. Kuwano Y, Spelten O, Zhang H, Ley K, Zarbock A. Rolling on E- or P-selectin induces the extended but not high-affinity conformation of LFA-1 in neutrophils. Blood. 2010;116:617–24.
19. Fan Z, et al. Neutrophil recruitment limited by high-affinity bent beta2 integrin binding ligand in cis. Nat Commun. 2016;7:12658.
20. Lawrence MB, Springer TA. Leukocytes roll on a selectin at physiologic flow rates: distinction from and prerequisite for adhesion through integrins. Cell. 1991;65:859–73.
21. DiVietro JA, et al. Immobilized IL-8 triggers progressive activation of neutrophils rolling in vitro on P-selectin and intercellular adhesion molecule-1. J Immunol. 2001;167:4017–25.
22. Wang Y, et al. The role of G protein-coupled receptor in neutrophil dysfunction during sepsis-induced acute respiratory distress syndrome. Front Immunol. 2023;14:1112196.
23. Wen L, Moser M, Ley K. Molecular mechanisms of leukocyte beta2 integrin activation. Blood. 2022;139:3480–92.
24. Bromberger T, et al. Binding of Rap1 and Riam to Talin1 Fine-Tune beta2 integrin activity during leukocyte trafficking. Front Immunol. 2021;12:702345.

25. Ni N, Kevil CG, Bullard DC, Kucik DF. Avidity modulation activates adhesion under flow and requires cooperativity among adhesion receptors. Biophys J. 2003;85:4122–33.
26. Stewart M, Hogg N. Regulation of leukocyte integrin function: affinity vs. avidity. J Cell Biochem. 1996;61:554–61.
27. Changede R, Sheetz M. Integrin and cadherin clusters: a robust way to organize adhesions for cell mechanics. BioEssays. 2017;39:1–12.
28. van Kooyk Y, Figdor CG. Avidity regulation of integrins: the driving force in leukocyte adhesion. Curr Opin Cell Biol. 2000;12:542–7.
29. Luo BH, Carman CV, Springer TA. Structural basis of integrin regulation and signaling. Annu Rev Immunol. 2007;25:619–47.
30. Alon R, Feigelson SW. Chemokine-triggered leukocyte arrest: force-regulated bi-directional integrin activation in quantal adhesive contacts. Curr Opin Cell Biol. 2012;24:670–6.
31. Ley K, Laudanna C, Cybulsky MI, Nourshargh S. Getting to the site of inflammation: the leukocyte adhesion cascade updated. Nat Rev Immunol. 2007;7:678–89.
32. Fan Z, et al. High-Affinity Bent beta(2)-Integrin molecules in arresting neutrophils face each other through binding to ICAMs in cis. Cell Rep. 2019;26:119–e130115.
33. Lefort CT, Ley K. Neutrophil arrest by LFA-1 activation. Front Immunol. 2012;3:157.
34. Lefort CT, et al. Distinct roles for talin-1 and kindlin-3 in LFA-1 extension and affinity regulation. Blood. 2012;119:4275–82.
35. Malinin NL, et al. A point mutation in KINDLIN3 ablates activation of three integrin subfamilies in humans. Nat Med. 2009;15:313–8.
36. Svensson L, et al. Leukocyte adhesion deficiency-III is caused by mutations in KINDLIN3 affecting integrin activation. Nat Med. 2009;15:306–12.
37. Sun H, et al. Frontline Science: a flexible kink in the transmembrane domain impairs beta2 integrin extension and cell arrest from rolling. J Leukoc Biol. 2020;107:175–83.
38. Moser M, et al. Kindlin-3 is required for beta2 integrin-mediated leukocyte adhesion to endothelial cells. Nat Med. 2009;15:300–5.
39. Wen L, et al. Kindlin-3 recruitment to the plasma membrane precedes high-affinity beta2-integrin and neutrophil arrest from rolling. Blood. 2021;137:29–38.
40. Anthis NJ, et al. The structure of an integrin/talin complex reveals the basis of inside-out signal transduction. EMBO J. 2009;28:3623–32.
41. Wegener KL, et al. Structural basis of integrin activation by talin. Cell. 2007;128:171–82.
42. Sun J, et al. Structure basis of the FERM domain of kindlin-3 in supporting integrin alphaIIbbeta3 activation in platelets. Blood Adv. 2020;4:3128–35.
43. Haydari Z, Shams H, Jahed Z, Mofrad MRK. Kindlin assists Talin to promote integrin activation. Biophys J. 2020;118:1977–91.
44. Simonson WT, Franco SJ, Huttenlocher A. Talin1 regulates TCR-mediated LFA-1 function. J Immunol. 2006;177:7707–14.
45. Franco SJ, et al. Calpain-mediated proteolysis of talin regulates adhesion dynamics. Nat Cell Biol. 2004;6:977–83.
46. Liu J, et al. Talin determines the nanoscale architecture of focal adhesions. Proc Natl Acad Sci U S A. 2015;112:E4864–4873.
47. Han SJ et al. Pre-complexation of talin and vinculin without tension is required for efficient nascent adhesion maturation. Elife. 2021;10:e66151.
48. Kumar A, et al. Talin tension sensor reveals novel features of focal adhesion force transmission and mechanosensitivity. J Cell Biol. 2016;213:371–83.
49. Walde M, Monypenny J, Heintzmann R, Jones GE, Cox S. Vinculin binding angle in podosomes revealed by high resolution microscopy. PLoS ONE. 2014;9:e88251.
50. Pernier J et al. Talin and Kindlin cooperate to control the density of integrin clusters. J Cell Sci. 2023;136(8):jcs260746.
51. Feigelson SW, et al. Kindlin-3 is required for the stabilization of TCR-stimulated LFA-1:ICAM-1 bonds critical for lymphocyte arrest and spreading on dendritic cells. Blood. 2011;117:7042–52.
52. Schmidt S, et al. Kindlin-3-mediated signaling from multiple integrin classes is required for osteoclast-mediated bone resorption. J Cell Biol. 2011;192:883–97.
53. Ye F, et al. The mechanism of kindlin-mediated activation of integrin alphaIIb-beta3. Curr Biol. 2013;23:2288–95.
54. Ley K, Rivera-Nieves J, Sandborn WJ, Shattil S. Integrin-based therapeutics: biological basis, clinical use and new drugs. Nat Rev Drug Discov. 2016;15:173–83.
55. Sai J, Walker G, Wikswo J, Richmond A. The IL sequence in the LLKIL motif in CXCR2 is required for full ligand-induced activation of Erk, akt, and chemotaxis in HL60 cells. J Biol Chem. 2006;281:35931–41.
56. Dransfield I, Hogg N. Regulated expression of Mg2 + binding epitope on leukocyte integrin alpha subunits. EMBO J. 1989;8:3759–65.
57. Robinson MK, et al. Antibody against the Leu-CAM beta-chain (CD18) promotes both LFA-1- and CR3-dependent adhesion events. J Immunol. 1992;148:1080–5.
58. Yang W, Shimaoka M, Chen J, Springer TA. Activation of integrin beta-subunit I-like domains by one-turn C-terminal alpha-helix deletions. Proc Natl Acad Sci U S A. 2004;101:2333–8.
59. Lu C, Ferzly M, Takagi J, Springer TA. Epitope mapping of antibodies to the C-terminal region of the integrin beta 2 subunit reveals regions that become exposed upon receptor activation. J Immunol. 2001;166:5629–37.
60. Bromberger T, Klapproth S, Sperandio M, Moser M. Humanized beta2 Integrin-Expressing Hoxb8 Cells Serve as Model to Study Integrin Activation. Cells. 2022;11(9):1532
61. Fan Z, Mikulski Z, McArdle S, Sundd P, Ley K. Super-STORM: Molecular modeling to achieve single-molecule localization with STORM Microscopy. STAR Protoc. 2020;1:100012.
62. Dempsey GT, Vaughan JC, Chen KH, Bates M, Zhuang X. Evaluation of fluorophores for optimal performance in localization-based super-resolution imaging. Nat Methods. 2011;8:1027–36.
63. Hu F, et al. Super-resolution microscopy reveals nanoscale architecture and regulation of podosome clusters in primary macrophages. iScience. 2022;25:105514.
64. Conley H, Till RL, Berglund AK, Jones SL, Sheats MK. A myristoylated alanine-rich C-kinase substrate (MARCKS) inhibitor peptide attenuates neutrophil outside-in beta(2)-integrin activation and signaling. Cell Adh Migr. 2023;17:1–16.
65. Morikis VA, Rivara K, Simon SI. Kinky integrins reveal a new wrinkle in neutrophil activation. J Leukoc Biol. 2020;107:167–9.
66. Chang CW, Cheng N, Bai Y, Skidgel RA, Du X. Galpha(13) mediates Transendothelial Migration of neutrophils by promoting integrin-dependent motility without affecting directionality. J Immunol. 2021;207:3038–49.
67. Theodosiou M, et al. Kindlin-2 cooperates with talin to activate integrins and induces cell spreading by directly binding paxillin. Elife. 2016;5:e10130.
68. Immler R, et al. The voltage-gated potassium channel KV1.3 regulates neutrophil recruitment during inflammation. Cardiovasc Res. 2022;118:1289–302.
69. Manevich-Mendelson E, et al. Loss of Kindlin-3 in LAD-III eliminates LFA-1 but not VLA-4 adhesiveness developed under shear flow conditions. Blood. 2009;114:2344–53.
70. Xu Z, Jobe SM, Ma YQ, Shavit JA. A novel LAD-III mutation manifests functional importance of the compact FERM domain in Kindlin-3. J Thromb Haemost. 2023; 22(2):558-564.
71. Koker N, et al. A novel deletion in FERMT3 causes LAD-III in a Turkish family. J Clin Immunol. 2023;43:741–6.
72. Kahraman AB, et al. Clinical and Osteopetrosis-Like Radiological findings in patients with Leukocyte Adhesion Deficiency Type III. J Clin Immunol. 2023;43:1250–8.
73. Szpak D, et al. Kindlin-3 deficiency leads to impaired erythropoiesis and erythrocyte cytoskeleton. Blood Adv. 2023;7:1739–53.
74. Hart R, Stanley P, Chakravarty P, Hogg N. The kindlin 3 pleckstrin homology domain has an essential role in lymphocyte function-associated antigen 1 (LFA-1) integrin-mediated B cell adhesion and migration. J Biol Chem. 2013;288:14852–62.
75. Orre T, et al. Molecular motion and tridimensional nanoscale localization of kindlin control integrin activation in focal adhesions. Nat Commun. 2021;12:3104.
76. Bu W, et al. Structural basis of human full-length kindlin-3 homotrimer in an auto-inhibited state. PLoS Biol. 2020;18:e3000755.
77. Ni T, et al. Structure and lipid-binding properties of the kindlin-3 pleckstrin homology domain. Biochem J. 2017;474:539–56.
78. Wen L, Lyu Q, Ley K, Goult BT. Structural Basis of beta2 Integrin Inside-Out Activation. Cells. 2022;11(19):3039.
79. Picas L, et al. BIN1/M-Amphiphysin2 induces clustering of phosphoinositides to recruit its downstream partner dynamin. Nat Commun. 2014;5:5647.
80. Wang Q, Pechersky Y, Sagawa S, Pan AC, Shaw DE. Structural mechanism for Bruton's tyrosine kinase activation at the cell membrane. Proc Natl Acad Sci U S A. 2019;116:9390–9.

81. Patra MC, Choi S. Insight into phosphatidylinositol-dependent membrane localization of the Innate Immune adaptor protein Toll/Interleukin 1 receptor domain-containing adaptor protein. Front Immunol. 2018;9:75.
82. Li Z, Venable RM, Rogers LA, Murray D, Pastor RW. Molecular dynamics simulations of PIP2 and PIP3 in lipid bilayers: determination of ring orientation, and the effects of surface roughness on a Poisson-Boltzmann description. Biophys J. 2009;97:155–63.
83. van den Bogaart G, et al. Membrane protein sequestering by ionic protein-lipid interactions. Nature. 2011;479:552–5.
84. Yamamoto E, et al. Multiple lipid binding sites determine the affinity of PH domains for phosphoinositide-containing membranes. Sci Adv. 2020;6:eaay5736.
85. Ran FA, et al. Genome engineering using the CRISPR-Cas9 system. Nat Protoc. 2013;8:2281–308.
86. Andronov L, Orlov I, Lutz Y, Vonesch JL, Klaholz BP. ClusterViSu, a method for clustering of protein complexes by Voronoi tessellation in super-resolution microscopy. Sci Rep. 2016;6:24084.
87. Levet F, et al. SR-Tesseler: a method to segment and quantify localization-based super-resolution microscopy data. Nat Methods. 2015;12:1065–71.

Publisher's note

Springer Nature remains neutral with regard to jurisdictional claims in published maps and institutional affiliations.